

Predictive Modelling to Study the Electrochemical Behaviour of PdO, TiO₂ and Perovskite-Type LaFeO₃ Modified Carbon Paste Electrodes

Douglas Vieira Thomaz¹, Adelmo Menezes de Aguiar Filho¹, Isaac Yves Lopes de Macedo¹, Edson Silvio Batista Rodrigues¹, Eric de Souza Gil¹

¹ Universidade Federal de Goiás

240 street, Leste Universitário district, Goiânia - GO, 74605-170, Brazil

DOI: [10.22178/pos.45-3](https://doi.org/10.22178/pos.45-3)


LCC Subject Category: [RM1-950](#)

Received 27.02.2019

Accepted 27.03.2019

Published online 30.04.2019

Corresponding Author:
Douglas Vieira Thomaz
douglasvthomaz@gmail.com

© 2019 The Authors. This article is licensed under a [Creative Commons Attribution 4.0 License](#) 

Abstract. Transition metals are highly sought after in electrode construction due to their eventual electrocatalytic effects. In this context, this work presents the study of several metal oxide modified electrodes focusing in the evaluation of their electrochemical features through voltammetry and Electrochemical Impedance Spectroscopy (EIS). Moreover, a predictive statistical model was also developed using LASSO regression. Henceforth, glassy carbon electrode (GCE) and carbon paste electrode (CPE) were used to establish correlations between the herein studied modifications, namely: PdO@CPE, TiO₂@CPE, and LaFeO₃@CPE. Results evidence that metal oxide modified electrodes may increase signal detection through electrocatalytic effects, however, the herein developed model evidenced that surface area plays a major role in electrode response through voltammetry.

Keywords: transition metal; electrochemical impedance spectroscopy; resistance; modified electrode.

INTRODUCTION

Electrode modification is an important element employed in electrochemistry, as it provides signal modulation and may allow better analytical performance. Under the light of electroanalytical chemistry, electrodes are employed to quantify drugs in pharmaceutical forms, as well as samples from a wide variety of sources. Moreover, these devices can also be used in biosensing technologies [1, 2]

Amidst the materials used in electrode design, Carbon Paste (CP) is often employed hence its easy preparation and low cost. Moreover, modifications are easily feasible through direct addition of modifying agents, which may be of either organic or inorganic nature. The use of CP electrodes can furthermore lead to higher reproducibility, as the surface is renewed prior to each analysis, therefore limiting the impact of electrode fouling [3, 4].

Among commonly employed compounds in electrode modifications, metal oxides are highly regarded due to their acidic behavior, which promotes analyte oxidation and henceforth, increased faradaic response when anodic scans are

concerned. Metal oxides are moreover prone to be adsorbed on CP surface, therefore providing quick electrode preparation, which requires few steps. These electrodes are used in the study of a myriad of analytes from both synthetic and natural origin, as well as applied on eletroremediation techniques [5, 6].

The study of electrode features provides valuable information concerning the electrochemical features of these devices. In this context, modifications are usually studied by methods such as voltammetry and impedimetry [7, 8]. Regarding the theoretical circuit design of an electrode, Electrochemical Impedance Spectroscopy (EIS) provides deep information on phase shifts and charge kinetics, henceforth turning this method into an optimal alternative to characterize the electrochemical features of many modifications [9, 10].

Since electrode characterization is essential to better understand the features of these devices, and theoretical calculus based on electrochemical parameters may be useful for predictive information, this work is intended to provide a comprehensive study of the electrochemical behavior of modified and non-modified electrodes.

Therefore, voltammetric and EIS analysis were conducted to assess particular features of Glassy Carbon Electrode (GCE); CPE; and CPE modified with metal oxides, namely: PdO; TiO₂ and Perovskite-Type LaFeO₃. Furthermore, statistical modeling was also used to establish a predictive study of electrode behavior.

MATERIAL AND METHODS

Reagents and Materials. Potassium ferrocyanide, KCl, Fe(NO₃)₃·9H₂O and La(CH₃COO)₃·1.5H₂O were purchased from Vetec Química Fina Ltda. (Rio de Janeiro, Brasil). Potassium ferrocyanide was diluted in purified water (conductivity ≤ 0.1 μS·cm⁻¹) obtained from Milli-Q purification system Millipore S/A (Molsheim, França) in order to reach a final concentration of 0.001 mol L⁻¹. Thereafter, KCl was added to this solution up to a concentration of 0.1 mol L⁻¹.

Mineral oil, Carbon graphite, Palladium oxide and Titanium IV Isopropoxide were purchased from (Sigma-Aldrich, St. Louis, MO, USA). Perovskite-Type LaFeO₃ herein employed was produced and characterized according to previously described protocol [4].

Electrode preparation. CPE was prepared through homogenization of a mixture of 100 mg carbon graphite and 30 mg of mineral oil (Lujol®), herein employed as agglutinating agent.

TiO₂ adsorbed carbon was produced according to the following protocol: 1.5 g of unmodified graphite powder was immersed and rigorously mixed in 30 ml of ethanol:acetone solution (1:1) at 30 °C for 10 minutes. Thereafter, 10 ml of ethanol:acetone solution (1:1) containing 1.3 % titanium IV isopropoxide was added to graphite suspension drop by drop during two hours. All other metal modifications were conducted following the same protocol and proportions, therefore, 10 ml of ethanol:acetone solution (1:1) containing 1.3 % of either Palladium oxide or Perovskite type LaFeO₃ was added to graphite suspension drop by drop during two hours.

All aforementioned procedures were conducted at 30 °C. The material was then dried in vacuum desiccator at 70 °C (Selecta heated vacuum desiccator "Vacuo-Temp", Spain).

Each metal modified material was mixed with unmodified graphite powder at a proportion of 1:1. Thereafter, 30 mg mineral oil was added to allow the formation of the carbon paste. All pro-

portions are listed in Table 1. The modifications herein employed were subjected to scanning electron microscopy and elemental characterization in previous works by our group [4, 5].

Table 1 – Electrode composition

Electrode	Carbon Graphite, mg	Metal Adsorbed Carbon, mg	Mineral oil, mg	Electrode surface área (mm ²)
GCE	-	-	-	4.58
CPE	100	-	30	7.77
PdO@CPE	50	50	30	5.86
TiO ₂ @CPE	50	50	30	5.43
LaFeO ₃ @CPE	50	50	30	8.06

Electrochemical Assays. EIS and Cyclic Voltammetry (CV) measurements were performed using a potentiostat/galvanostat PGSTAT® model 204 with FRA32M module (MetrohAutolab) integrated with NOVA 2.1® software. All measurements were performed in 1 ml one-compartment electrochemical cell coupled to a three-electrode system consisting of the working electrodes described in Table 1, Pt wire and Ag/AgCl/KCl_{sat} (both purchased from Lab solutions, São Paulo, Brazil). The electrodes cited above represent: working, counter and reference electrode, respectively.

EIS measurements were conducted in a solution containing 0.001 mol L⁻¹ potassium ferrocyanide and 0.1 mol L⁻¹ KCl over a frequency ranging from 0.01 Hz to 100 KHz at selected potentials for all tested electrodes.

The experimental conditions for CV were: scan rate (v) of either: 12.5; 25; 50; 100; 250 or 500 mV s⁻¹, and scan range of -0.5 to 1.0. All experiments were performed at room temperature (21 ± 2 °C) in triplicates (n = 3) in 0.001 mol L⁻¹ potassium ferrocyanide / 0.1 mol L⁻¹ KCl solution.

Plots of the voltammetric curves for final presentation in this study were drawn using Origin Pro 8® software (Northampton, MA, USA).

Statistical Modelling. In order to establish a statistical model to the herein studied electrodic features a lasso regression was fitted to interpretate the effect and signal of the main electrode characterization variables in the anodic signals taken from CV scans (Figure 1).

LASSO (Least Absolute Shrinkage and Selection Operator) is a shrinkage linear regression that

shrinks model coefficients in order to obtain a generalized behavior of all phenomena in the system.

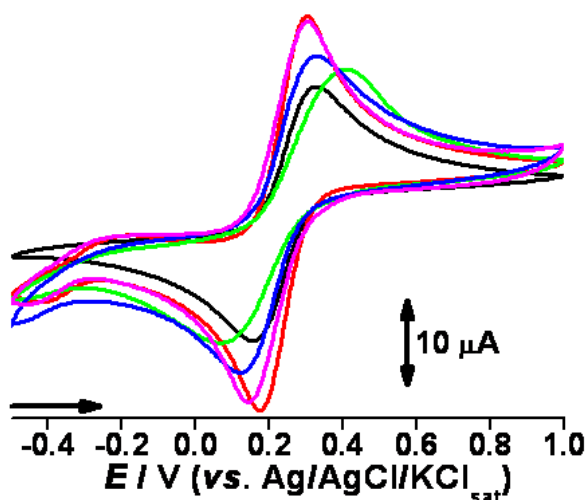


Figure 1 – Cyclic voltammograms taken from ferrocyanide solution using different electrodes

Notes: Black – GCE; Red – CPE; Green – PdO@CPE; Blue – TiO₂@CPE; Magenta – LaFeO₃@CPE.

All analysis carried out at ν of 100 mV s⁻¹ in 0.001 mol L⁻¹ potassium ferrocyanide/0.1 mol L⁻¹ KCl.

It was chosen due to its main features, which overpasses the main drawbacks of classic linear models (variable correlation, need for high n , and etc) [11].

All statistical analysis was conducted in R software [12].

RESULTS AND DISCUSSION

CV and EIS Assays. In order to preliminarily assess their response, electrodes were subjected to CV in a diffusion controlled environment i.e. potassium ferrocyanide/KCl solution. GCE was used as a control (Black color) in order to compare the influence of the herein employed modifications. Results are displayed in Figure 1.

Results indicate that modifications increase sensibility towards faradaic current detection, as metal modified electrodes presented higher anodic peaks, I_{pa} , than bare GCE. The same can be stated about the cathodic peaks, I_{pc} , whose amplitude increased when modified electrodes were employed. This result is in consonance with literature, which reports that transition metals promote electrocatalytic oxidation of analytes,

henceforth increasing their faradaic signals [10, 11].

An interesting finding is that unmodified CPE presented higher signal than that of bare GCE (Figure 1). Since this result suggests that factors other than metal oxide presence in electrode matrix may influence sensibility, electrode surface area was calculated. Therefore, anodic peak currents were taken from voltammograms recorded at different scan rates using all modified electrodes. Both unmodified CPE and modified electrodes were analyzed, namely: PdO@CPE; TiO₂@CPE and LaFeO₃@CPE. Results are displayed in Figure 2.

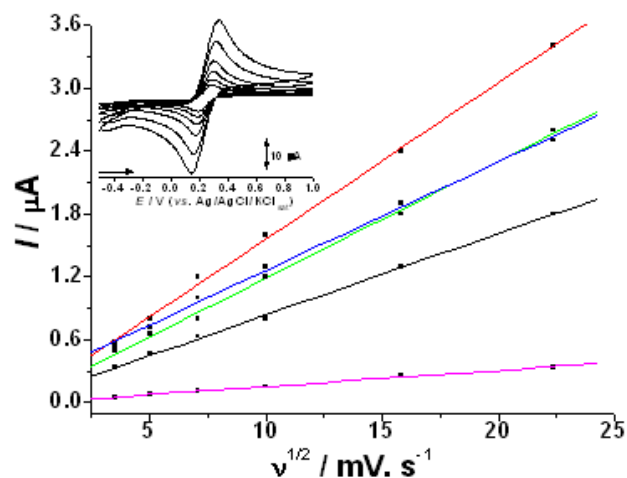


Figure 2 – Plot of peak current (I) vs scan rate square root ($\nu^{1/2}$)

Notes: Black – GCE; Red – CPE; Green – PdO@CPE; Blue – TiO₂@CPE; Magenta – LaFeO₃@CPE.

Cyclic voltammogram representation of ferrocyanide solution at different scan rates (12.5, 25, 50, 100, 250 and 500 mV s⁻¹) at GCE. All analysis carried out in 0.001 mol L⁻¹ potassium ferrocyanide/0.1 mol L⁻¹ KCl.

All plots presented linear tendency between data from faradaic current peaks and scan rate's square root (Figure 2), which is in accordance with literature and experimental conditions, since data was taken in a diffusion controlled environment [14, 15]. Moreover, electrode surface area was determined by Randles-Sevcik equation (1), using 0.001 mol L⁻¹ potassium ferrocyanide and 0.1 mol L⁻¹ KCl as reversible one-electron diffusion controlled redox system.

$$I_{pa} = 2.69 \cdot 10^5 \text{ A } n^{3/2} D^{1/2} c \nu^{1/2} \quad (1)$$

where I_{pa} is the anodic peak current; A is electrode area in cm^2 , n is the number of transferred electrons; D is the diffusion coefficient, which was estimated to be $7.09 \cdot 10^{-6} \text{ cm}^2 \text{ s}^{-1}$ [14]; c is the concentration of potassium ferrocyanide/KCl in mol L^{-1} ; ν is scan rate in V s^{-1} .

The values of $I_{pa}/\nu^{1/2}$ were obtained from the slopes of the curves displayed in Figure 2. All calculated electrode surface areas are displayed in Table 1.

The calculated surface areas of the electrodes evidenced that all CP based electrodes presented

higher surface area than GCE (Table 1), which in turn promoted the detection of higher current densities (Figure 1) [17, 18]. Moreover, the proposed electrocatalytic effect did not seem to increase electrode sensibility in any of the studied modifications [17, 19].

Given that GCE and CPE are the only unmodified electrodes herein employed, they were subjected to EIS to evaluate their impedance. Results are displayed in Figure 3A. EIS was also conducted on all modified electrodes. Results are displayed in Figure 3B.

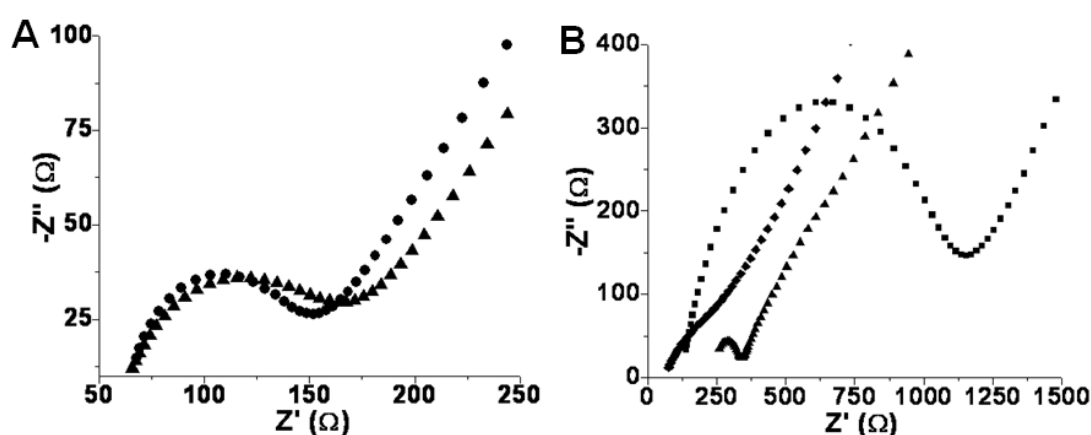


Figure 3 – EIS nyquist plot

Notes: 3A) EIS nyquist plot of GCE (●) and CPE (▲); 3B) EIS nyquist plot of PdO@CPE (■), TiO₂@CPE (◆) and LaFeO₃@CPE (▲).

All analysis carried out in 0.001 mol L^{-1} potassium ferrocyanide/ 0.1 mol L^{-1} .

Since circuit parameters are essential to better understand electrode behavior, all data concerning the Randles equivalent circuit of each electrode was gathered and displayed in Table 2, where R_s is uncompensated ohmic resistance (Ω); R_{ct} represents the resistance associated to charge transfer (Ω); C and n are respectively the pseudo-capacitance (μF) and frequency independent taken from the constant phase element, which describes the imperfect capacitive behavior of the double-layer.

Table 2 – Randles equivalent circuit elements for each electrode

Electrode	Circuit elements	Circuit elements
GCE	R_s	59
	R_{ct}	120
	n	0.707
	C	1.330

Electrode	Circuit elements	Circuit elements
CPE	R_s	58
	R_{ct}	114
	n	0.792
	C	2.320
PdO@CPE	R_s	124
	R_{ct}	102
	n	0.732
	C	1.080
TiO ₂ @CPE	R_s	54.5
	R_{ct}	524
	n	0.381
	C	7.470
LaFeO ₃ @CPE	R_s	499
	R_{ct}	152
	n	0.184
	C	0.002

The values taken from each equivalent Randles circuit evidence that TiO_2 and LaFeO_3 modifications increase the resistive character on the electrodes, as n values were close to 0, which implies the behavior of an ideal resistor. Such trend was not followed by GCE, CPE and PdO modified electrodes, which presented n values closer to 1, characteristic of an ideal capacitor (Table 2).

Results evidenced that GCE presents similar impedance profile to that of CPE. Moreover, CPE impedance showed higher $-Z''$ (imaginary impedance) throughout the near end of the semi-circle, in comparison with GCE, thus, double layer capacitance kept higher in lower frequencies (Figure 3A). This trend was confirmed through the pseudo-capacitance value of CPE, which was nonetheless superior to that of GCE, therefore confirming that CPE presents greater capacitive behavior (Table 2).

These results are further corroborated by the calculated electrode surface area, which evidenced that CPE presents higher surface area than GCE (Table 1). Since electrode surface area is directly proportional to double layer area as well as capacitive behavior, the herein exhibited findings are in consonance to literature data [20, 21].

EIS results show moreover that each metal modification deeply influenced impedance values of circuit elements, which is nonetheless in accordance to literature [9, 22]. PdO modification promoted higher capacitive behavior, whereas TiO_2 and Perovskite-type LaFeO_3 did not follow the same trend (Figure 3B).

Circuit data presents both TiO_2 @CPE and LaFeO_3 @CPE as the least capacitive, which is remarkable, since solid electrodes tend to exhibit capacitive behavior [9, 23]. LaFeO_3 @CPE presented moreover the highest surface area, which would implicate in greater capacitance (Table 1) [24, 25]. Results suggest therefore that electrode matrix may also influence double layer features, being this finding corroborated by literature [24, 26].

Statistical Model. The fitted model presented statistical significance ($r^2 = 0.830$, $p < 0.05$) to predict the peak currents seen in CV through electrode element values taken from Randles theoretical circuit in EIS (Figure 4).

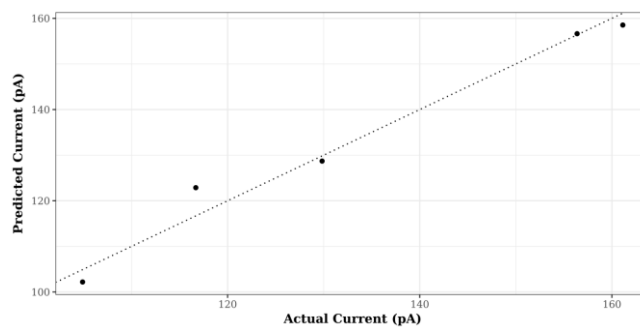


Figure 4 – Predicted against actual current peak taken from CV scans

Furthermore, the model presented Gaussian distribution of residues (Shapiro-Wilk, $p > 0.005$) [27], and the coefficients of the fitted LASSO regression, which are shown in Table 3, implicate in the influence displayed by each circuit component in the anodic peak amplitude seen in CV.

Table 3 – Lasso regression coefficients

R_s	R_{ct}	n	Electrode surface area
-24.769	-8.033	-21.258	30.267

The model implicate that both R_s and R_{ct} negatively affect peak amplitude, which is in accordance to literature data. Resistance of circuit components decreases current density, and the n value, which is correlated to the electrode resistive or capacitive behavior, also promotes the same effect in the herein developed model [23, 24]. Moreover, C value was not taken, as the pseudo-capacitance is intimately related to the calculated constant phase element and therefore n value in EIS [9].

Electrode surface area exhibited positive effect towards peak amplitude values taken from CV scans, which is in consonance to literature. The increment of surface area in electrodes tends to furthermore both increase capacitance as well as current density, being the later effect herein seen, and the one which nonetheless exhibited highest influence in peak amplitude, and therefore electrode sensibility [17, 18].

CONCLUSION

The present work studied the features of GCE, CPE and several metal modified CPE, namely: PdO; TiO_2 ; and perovskite-type LaFeO_3 .

Results evidence that electrode matrix does indeed influence probe detection through electro-catalytic effect. Moreover, the herein developed

model evidenced that surface area plays a major role in electrode response through voltammetry.

REFERENCES

1. Ratajczak, P., Suss, M. E., Kaasik, F., & Béguin, F. (2019). Carbon electrodes for capacitive technologies. *Energy Storage Materials*, 16, 126–145. doi: [10.1016/j.ensm.2018.04.031](https://doi.org/10.1016/j.ensm.2018.04.031)
2. Simonet, J. (2018). Electrochemical carboxylation of titanium to generate versatile new interfaces. *Electrochemistry Communications*, 88, 67–70. doi: [10.1016/j.elecom.2018.01.007](https://doi.org/10.1016/j.elecom.2018.01.007)
3. Antunes, R., Ferraz, D., Garcia, L., Thomaz, D., Luque, R., Lobón, G., ... Lopes, F. (2018). Development of a Polyphenol Oxidase Biosensor from Jenipapo Fruit Extract (*Genipa americana* L.) and Determination of Phenolic Compounds in Textile Industrial Effluents. *Biosensors*, 8(2), 47. doi: [10.3390/bios8020047](https://doi.org/10.3390/bios8020047)
4. De Macedo, I. Y. L., Garcia, L. F., de Souza, A. R., da Silva, A. M. L., Fernandez, C., Santos, M. D. G., ... Gil, E. de S. (2016). Differential Pulse Voltammetric Determination of Albendazole and Mebendazole in Pharmaceutical Formulations Based on Modified Sonogel Carbon Paste Electrodes with Perovskite-Type LaFeO₃Nanoparticles. *Journal of The Electrochemical Society*, 163(8), B428–B434. doi: [10.1149/2.0661608jes](https://doi.org/10.1149/2.0661608jes)
5. Sanz, G., Ferreira Garcia, L., Yopez, A., Colletes de Carvalho, T., Gontijo Vaz, B., Romão, W., ... Luque, R. (2018). TiO₂@C Nanostructured Electrodes for the Anodic Removal of Cocaine. *Electroanalysis*, 30(9), 2094–2098. doi: [10.1002/elan.201800297](https://doi.org/10.1002/elan.201800297)
6. De Oliveira Neto, J. R., Rezende, S. G., Lobón, G. S., Garcia, T. A., Macedo, I. Y. L., Garcia, L. F., ... de Souza Gil, E. (2017). Electroanalysis and laccase-based biosensor on the determination of phenolic content and antioxidant power of honey samples. *Food Chemistry*, 237, 1118–1123. doi: [10.1016/j.foodchem.2017.06.010](https://doi.org/10.1016/j.foodchem.2017.06.010)
7. Sánchez-Calvo, A., Núñez-Bajo, E., Fernández-Abedul, M. T., Blanco-López, M. C., & Costa García, A. (2018). Optimization and characterization of nanostructured paper-based electrodes. *Electrochimica Acta*, 265, 717–725. doi: [10.1016/j.electacta.2018.01.179](https://doi.org/10.1016/j.electacta.2018.01.179)
8. Carneiro, M. C. C. G., Moreira, F. T. C., Dutra, R. A. F., Fernandes, R., & Sales, M. G. F. (2018). Homemade 3-carbon electrode system for electrochemical sensing: Application to microRNA detection. *Microchemical Journal*, 138, 35–44. doi: [10.1016/j.microc.2017.12.026](https://doi.org/10.1016/j.microc.2017.12.026)
9. De Oliveira, F. M., de J. Guedes, T., Lima, A. B., Da Silva, L. M., & dos Santos, W. T. P. (2017). Alternative method to obtain the Tafel plot for simple electrode reactions using batch injection analysis coupled with multiple-pulse amperometric detection. *Electrochimica Acta*, 242, 180–186. doi: [10.1016/j.electacta.2017.05.018](https://doi.org/10.1016/j.electacta.2017.05.018)
10. Banerjee, S., Debata, S., Madhuri, R., & Sharma, P. K. (2018). Electrocatalytic behavior of transition metal (Ni, Fe, Cr) doped metal oxide nanocomposites for oxygen evolution reaction. *Applied Surface Science*, 449, 660–668. doi: [10.1016/j.apsusc.2017.12.014](https://doi.org/10.1016/j.apsusc.2017.12.014)
11. Tibshirani, R. (2011). Regression shrinkage and selection via the lasso: a retrospective. *Journal of the Royal Statistical Society: Series B (Statistical Methodology)*, 73(3), 273–282. doi: [10.1111/j.1467-9868.2011.00771.x](https://doi.org/10.1111/j.1467-9868.2011.00771.x)
12. R Foundation for Statistical Computing. (2018). *R: A language and environment for statistical computing*. Retrieved from <http://softlibre.unizar.es/manuales/aplicaciones/r/fullrefman.pdf>
13. Akbari, A., Amini, M., Tarassoli, A., Eftekhari-Sis, B., Ghasemian, N., & Jabbari, E. (2018). Transition metal oxide nanoparticles as efficient catalysts in oxidation reactions. *Nano-Structures & Nano-Objects*, 14, 19–48. doi: [10.1016/j.nanoso.2018.01.006](https://doi.org/10.1016/j.nanoso.2018.01.006)

14. Hrdlička, V., Navrátil, T., Barek, J., & Ludvík, J. (2018). Electrochemical behavior of polycrystalline gold electrode modified by thiolated calix[4]arene and undecanethiol. *Journal of Electroanalytical Chemistry*, 821, 60–66. doi: [10.1016/j.jelechem.2018.01.055](https://doi.org/10.1016/j.jelechem.2018.01.055)
15. Mooste, M., Kibena-Põldsepp, E., Marandi, M., Matisen, L., Sammelseg, V., Podvorica, F. I., & Tammeveski, K. (2018). Surface and electrochemical characterization of aryl films grafted on polycrystalline copper from the diazonium compounds using the rotating disk electrode method. *Journal of Electroanalytical Chemistry*, 817, 89–100. doi: [10.1016/j.jelechem.2018.03.070](https://doi.org/10.1016/j.jelechem.2018.03.070)
16. Konopka, S. J., & McDuffie, B. (1970). Diffusion coefficients of ferri- and ferrocyanide ions in aqueous media, using twin-electrode thin-layer electrochemistry. *Analytical Chemistry*, 42(14), 1741–1746. doi: [10.1021/ac50160a042](https://doi.org/10.1021/ac50160a042)
17. Sun, S., Li, H., & Xu, Z. J. (2018). Impact of Surface Area in Evaluation of Catalyst Activity. *Joule*, 2(6), 1024–1027. doi: [10.1016/j.joule.2018.05.003](https://doi.org/10.1016/j.joule.2018.05.003)
18. Ye, Z., & Noréus, D. (2016). Metal hydride electrodes: The importance of surface area. *Journal of Alloys and Compounds*, 664, 59–64. doi: [10.1016/j.jallcom.2015.12.170](https://doi.org/10.1016/j.jallcom.2015.12.170)
19. Oliveira, L. S., Alba, J. F. G., Silva, V. L., Ribeiro, R. T., Falcão, E. H. L., & Navarro, M. (2018). The effect of surface functional groups on the performance of graphite powders used as electrodes. *Journal of Electroanalytical Chemistry*, 818, 106–113. doi: [10.1016/j.jelechem.2018.04.022](https://doi.org/10.1016/j.jelechem.2018.04.022)
20. Zhang, Q., Liu, X., Yin, L., Chen, P., Wang, Y., & Yan, T. (2018). Electrochemical impedance spectroscopy on the capacitance of ionic liquid–acetonitrile electrolytes. *Electrochimica Acta*, 270, 352–362. doi: [10.1016/j.electacta.2018.03.059](https://doi.org/10.1016/j.electacta.2018.03.059)
21. Uddin, M. S., Tanaya Das, H., Maiyalagan, T., & Elumalai, P. (2018). Influence of designed electrode surfaces on double layer capacitance in aqueous electrolyte: Insights from standard models. *Applied Surface Science*, 449, 445–453. doi: [10.1016/j.apsusc.2017.12.088](https://doi.org/10.1016/j.apsusc.2017.12.088)
22. Petovar, B., Khanari, K., & Finšgar, M. (2018). A detailed electrochemical impedance spectroscopy study of a bismuth-film glassy carbon electrode for trace metal analysis. *Analytica Chimica Acta*, 1004, 10–21. doi: [10.1016/j.aca.2017.12.020](https://doi.org/10.1016/j.aca.2017.12.020)
23. Ratajczak, P., Suss, M. E., Kaasik, F., & Béguin, F. (2019). Carbon electrodes for capacitive technologies. *Energy Storage Materials*, 16, 126–145. doi: [10.1016/j.ensm.2018.04.031](https://doi.org/10.1016/j.ensm.2018.04.031)
24. Pifferi, V., Rimoldi, L., Meroni, D., Segrado, F., Soliveri, G., Ardizzone, S., & Falciola, L. (2017). Electrochemical characterization of insulating silica-modified electrodes: Transport properties and physicochemical features. *Electrochemistry Communications*, 81, 102–105. doi: [10.1016/j.elecom.2017.06.014](https://doi.org/10.1016/j.elecom.2017.06.014)
25. Maccarrone, F., & Paffuti, G. (2018). Capacitance and forces for thick circular electrodes. *Journal of Electrostatics*, 94, 30–37. doi: [10.1016/j.elstat.2018.05.003](https://doi.org/10.1016/j.elstat.2018.05.003)
26. Uddin, M. S., Tanaya Das, H., Maiyalagan, T., & Elumalai, P. (2018). Influence of designed electrode surfaces on double layer capacitance in aqueous electrolyte: Insights from standard models. *Applied Surface Science*, 449, 445–453. doi: [10.1016/j.apsusc.2017.12.088](https://doi.org/10.1016/j.apsusc.2017.12.088)
27. Lockhart, R., Taylor, J., Tibshirani, R. J., & Tibshirani, R. (2014). Rejoinder: “A significance test for the lasso.” *The Annals of Statistics*, 42(2), 518–531. doi: [10.1214/14-aos1175rej](https://doi.org/10.1214/14-aos1175rej)